A novel 3D evaluation method for assessing bone to bone relationships in clubfoot

B. GANESAN[1,2,3], J. YIP[2], A. AL-JUMAILY[1], S.S.M. FONG[3], S. KOTHE BALASANKAR[4], A.M. EY BATLLE[5], K.N.K. FONG[6], A. LUXIMON[2]

[1]School of Biomedical Engineering, FEIT, University of Technology Sydney, Ultimo, NSW, Australia
[2]Institute of Textiles and Clothing, The Hong Kong Polytechnic University, Hung Hom, Hong Kong
[3]School of Public Health, Li Ka Shing Faculty of Medicine, The University of Hong Kong, Hong Kong, Hong Kong
[4]Maharashtra University of Health Sciences, Nashik, India
[5]Orthopaedics and Traumatology, Hospital Sant Joan De Deu, Barcelona, Spain
[6]Department of Rehabilitation Sciences, The Hong Kong Polytechnic University, Hung Hom, Hong Kong

Abstract. – OBJECTIVE: Clubfoot is a complex congenital three-dimensional foot deformity, which affects 150,000-200,000 newborn babies annually around the world. A good understanding of the alignment of the two osseous columns and the lower leg of the ankle and foot complex is essential for evaluating the severity of clubfoot. The purposes of this study were to (1) develop an automated three-dimensional (3D) surface model of severe clubfoot based on two-dimensional (2D) slices of computed tomography (CT) images, (2) evaluate the alignment of foot bones relative to the ankle in severe clubfoot, and (3) examine the structural changes in the shape of the clubfoot.

PATIENTS AND METHODS: Two-dimensional CT image was taken from a four-year-old child with a severe clubfoot. Subsequently, an automated and detailed 3D surface model of the severe clubfoot was developed from the 2D images by using MATLAB software programming. Then, the x, y, and z coordinate angles were automatically calculated for each bone in the foot relative to the ankle (lower end of the tibia) to determine the orientations and relationships among the bones.

RESULTS: The relative position or orientation of each bone of the foot to the ankle of the severe clubfoot was objectively measured which was used to determine the orientation of each bone in the foot. Among the x, y, and z axes of the interested tarsal bones, the z axis represents the smallest moment of inertia, and the results showed that the bones in the x axis shifted medially with higher relative angle.

CONCLUSIONS: This 3D objective measurement method for assessing clubfoot can be used to determine and classify the severity of clubfoot, as well as evaluate and monitor the progress of the clubfoot intervention based on the relative position of the tarsal bones. The method can also be used to quantify the relationship between the tarsal bones of the foot and lower end of the tibia. In addition, angular measurements can be used to assess other pathological conditions of the foot such as pes cavus and pes planus.

Key Words:
Clubfoot, 3D evaluation, Bone to bone evaluation, Clubfoot 3D-Model.

Introduction

Clubfoot is a three-dimensional (3D) musculoskeletal foot deformity that affects 150,000-200,000 newborn babies annually around the world[1]. This condition is characterized by four types of foot deformities: midfoot cavus, forefoot adductus, and hindfoot varus and equinus[2-4]. The evaluation of the anatomical structure and alignment of the tarsal bones is essential for understanding the severity and structural changes of clubfoot. A number of methods have been used to evaluate clubfoot deformity, such as clinical, radiological, functional, biomechanical, and imaging methods (computed tomography (CT), ultrasound (US), and magnetic resonance imaging (MRI)[5-10]. However, none of the methods are accepted as a universal assessment tool for evaluating severity of clubfoot[7,11-13].

The anatomical structural changes of clubfoot have been widely discussed in previous literature. For example, malalignment of the tarsal bones, joints, ligaments and other soft tissues[14-19], changes in alignment of talonavicular joint[5,9] and atypical morphology of talus[20]. Cahuzac et al[21] examined the osseous and cartilaginous relationships of ta-

Corresponding Authors: Balasankar Ganesan, Ph.D; e-mail: Balasankar.Ganesan@student.uts.edu.au
Joanne Yip, Ph.D; joanne.yip@polyu.edu.hk ▪ Adel Al-Jumaily, Ph.D; Adel.Al-Jumaily@uts.edu.au

lus and calcaneus bones in clubfoot. Ippolito et al[22] used volumetric magnetic resonance imaging (VMRI) and found differences in the volume and length of three muscle compartments (anterior, lateral and postero-medial muscular compartments) in the lower limb with a clubfoot deformity. Bhargava et al[23] applied US to explore the medial displacement of navicular in relation to head of talus; thickness of soft tissue in the medial and posterior aspects of foot; position of the neck and head of talus; distance between the calcaneus and cuboid, calcaneus, and length of the talus; distance between the calcaneus-ossification centre and the metaphysis of tibia; and Achilles tendon. Kruse et al[24] found an absence of posterior tibial artery in a magnetic resonance angiography test of the lower leg vasculatures. Some studies have investigated the length of the tibia and fibula along with the muscles, soft tissues, and anomalies of the arteries in clubfoot[25,26], and calculated the tibiofibular torsion angle[27]. Some of the biomechanical studies have also described the involvement of joints in the foot and osseous columns in clubfoot deformities. For example, talus, navicular, calcaneus, and cuboid bones are directly related to adductus, cavus, and varus deformities, especially at the mid-tarsal joints[18]. Equinus deformity usually occurs at talocrural and talonavicular joints, and forefoot[14]. Anatomically, ankle joint includes three joints, namely subtalar (talocalcaneal), talocrural (tibiotalar) and transverse-tarsal (talocalcaneonavicular) joints[28]. The talus, navicular, three cuneiforms, and first three metatarsals bones are in the medial osseous column, while the calcaneus, cuboids, and fourth and fifth metatarsals are located in the lateral osseous column. Abnormalities of the osseous columns and bones of the ankle joint are commonly seen in clubfoot deformity[29]. Therefore, a thorough understanding of the alignment of bones of the medial and lateral osseous columns, and lower leg of the ankle and foot complex is essential for evaluating the severity of clubfoot.

Previous imaging studies[22,30-32] have employed objective measurement methods to measure different angles, such as the anteroposterior talocalcaneal and calcaneocuboid angles, to determine the severity of the clubfoot. CT imaging also provides a better understanding of the abnormalities of the size and shape of the tarsal bones such as talus and calcaneus, and other tarsal bones. However, to the best of our knowledge, there are no studies that have examined each bone-to-bone relationships in the foot and ankle complex, and the bone-to-bone position in relation to the hindfoot, midfoot, and forefoot bones of the clubfoot. Specifically, alignment/position of the tarsal bones of the foot (talus, calcaneus, cuboid, metatarsal, and proximal and distal phalanges) in relation to the bones of the lower leg (tibia and fibula of the ankle joint region/ankle mortise) have not been examined so far. In addition, very few studies have utilized CT scanning to assess the progress of clubfoot associated with intervention or developed a 3D model of clubfoot from CT scans. Therefore, the purposes of this study was to develop a new 3D bone-to-bone evaluation method for quantifying clubfoot, and increase our understanding on the relative position of the tarsal bones to the foot and ankle complex, and evaluate "abnormal" arrangements of the bones of the ankle and foot complex, and develop a 3D model of bones in clubfoot from two-dimensional (2D) slices of scanned CT images.

Patients and Methods

Patients

A CT scan of a severe clubfoot of a four-year-old boy was used to develop the 3D surface model of clubfoot. Written informed consent was obtained from the parent of the child before starting the experiment. A Lightspeed 8 Ultra CT scanner (GE Healthcare Technologies, Waukesha, WI, USA) was used to obtain the 2D slices of the clubfoot images. The CT scanning parameters are: CT dose (CTD) volume – 1.71 mGy, tube voltage 100 KV, tube current – 23 mA and section thickness – 2.5 mm. The following five-step procedures were followed to evaluate the bone-to-bone relationships: the 2D slices were acquired, the noise from the 2D slices was aligned and removed, the images were then processed with MATLAB, a 3D model was developed for the bones of the clubfoot and the alignment of foot and ankle bones was analyzed (Figure 1). In the first step of developing the 3D model, the noise in the images (information of patient, CTD volume, tube voltage and current, section thickness, and lines between and under the images) was manually removed, and then the centre of the bone was marked by using a red dot in each 2D slice of an image to align the bone.

Three-Dimensional Modelling of Clubfoot

The aligned 2D slice images were imported into MATLAB R2017a (MathWorks Inc., 2017) to develop a 3D model of the clubfoot and analyse the bone-to-bone relationships. The red dots in

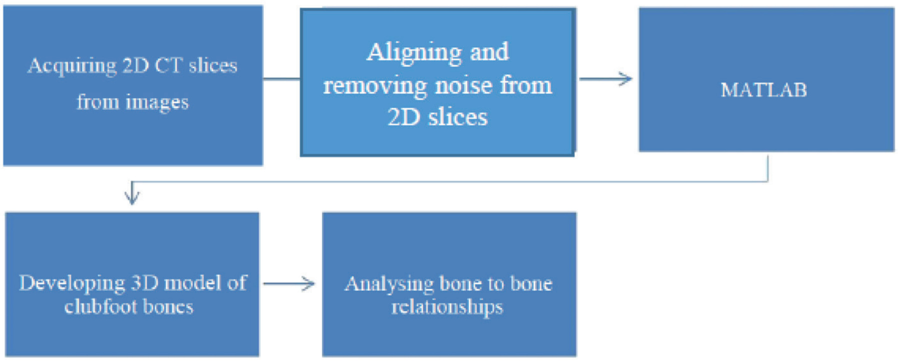

Figure 1. Framework for developing 3D model of clubfoot bones and analysing severe clubfoot.

the aligned 2D slices were merged together into red-dotted lines to identify each bone of the foot. Then, the MATLAB program was used to select the landmarks in the x, y, and z coordinate system (xyz vectors). This would automatically create 3D models of the foot (stereolithography (STL)) based on the position of the landmarks of the lower end of the tibia of the ankle region, fibula and the bones of interest in the foot. To develop the STL file (3D format) of the 3D model of the clubfoot bones, five landmarks points (green color) were selected as shown in Figure 2. The first point selected was at the lower end of tibia. The second and third points were at the lower end of fibula and lower part of tibia, respectively. The fourth and fifth points were at the proximal and distal ends of the bones of interest, which were calcaneus, cuboid, metatarsals, and proximal and distal phalanges. These points outlined the alignment and position of the foot in relation to the lower leg.

Next, a 3D model of the bones of the clubfoot was created in STL format as shown in Figure 2. The STL format allows the bones to be viewed or rotated in different 3D views such as YZ view (90, 0), XY view (0, 90), and XZ view (0, 0). The relationships among the orientations of the bones of interest with the lower leg bones (tibia and fibula) are described by using the x, y, and z Cardan angles. The angles were calculated for the bones of interest from their relative orientation to the tibia. In this study, Cardan angles for the tibia and the first, second, third, fourth and fifth metatarsals, and tibia the proximal, middle, and distal phalangeal bones were calculated to observe their position and alignment with the lower leg, and determine the severity of the clubfoot. More importantly, Cardan angles of the specific bones involved in the clubfoot such as the tibia-calcaneus, tibia-cuboid, tibia-talus, tibia-proximal, and middle, distal phalangeal bones were calculated to determine their relationships and orientations.

Results

Malalignment of tarsal bones is very common in clubfoot, which leads to four types of foot deformities, namely midfoot cavus, forefoot adductus, and hindfoot varus and equinus. It is difficult to describe them objectively due to the complexity of their anatomical structures and shape of the clubfoot. Therefore, an objective measurement method was developed in this study by using a semi-automated 3D model of the clubfoot bones to determine the clubfoot severity by analysing the bone-to-bone relationships. The lower end of tibia was used as a centre of the axis landmark (X axis), to objectively and quantitatively determine the orientation of each foot bone. The results of the x, y, z angles of each bone of interest in the foot were determined in relation to the tibia (Table I and II) as shown in Figure 3.

Table I. Calculation of angle of calcaneus, talus and cuboid bones in severe clubfoot.

Bone relationship	Angle X	Angle Y	Angle Z
Calcaneus relative to lower end of tibia	84.53	113.82	24.51
Talus relative to lower end of tibia	89.10	99.28	9.32
Cuboid relative to lower end of tibia	98.83	93.23	9.41

Table II. Alignment of metatarsal, proximal, middle, and distal phalanges relative to tibia (Ankle).

Bone Relationship	Angle X	Angle Y	Angle Z
Angles at metatarsal (MT) bone in relation to tibial bone			
First MT	74.77	46.34	47.61
Second MT	73.88	45.76	48.66
Third MT	68.39	48.79	49.00
Fourth MT	67.59	56.68	41.94
Fifth MT	68.31	69.81	30.37
Angles at proximal phalanges (PP) in relation to tibia or ankle			
First PP	62.53	68.71	35.93
Second PP	56.54	86.35	33.70
Third PP	55.60	80.07	36.19
Fourth PP	64.28	75.33	30.15
Fifth PP	50.87	91.02	39.14
Angles at middle phalanges (MP) in relation to tibia or ankle			
Second MP	56.32	67.38	42.44
Third MP	70.91	41.08	55.24
Fourth MP	72.74	47.19	47.85
Fifth MP	98.05	87.18	8.53
Angles at distal phalanges (DP) in relation to tibia or ankle			
First DP	68.95	90.60	21.05
Second DP	112.86	48.69	49.99
Third DP	106.07	96.15	17.26
Fourth DP	89.56	73.66	16.34
Fifth DP	65.47	76.64	28.36

Measuring Alignment of Talus, Calcaneus and Cuboid Bones Relative to Lower End of Tibia

Tarsal bones including calcaneus, cuboid and navicular bones, and the first, second, and third cuneiforms in the clubfoot were rotated in an inward direction in relation to the lower end of tibia and fibula. The calcaneus bone contributed to all four types of clubfoot deformities (midfoot cavus, forefoot adductus, and hindfoot varus and equinus). The cuboid bone shifted medially along with the anterior part of calcaneus[14]. The results of x, y, and z coordinate angles of the calcaneus, talus, and cuboid bones show the position of these bones relative to the tibia (Table I). The relative angles of the calcaneus, talus, and cuboid bones are shown in Figure 3b, 3c and 3d, respectively, in the x, y, and z directions. Among the x, y, and z axes of the tarsal bones of interest (i.e., the calcaneus, talus, and cuboid bones), the z axis represents the smallest moment of inertia as shown in Table I. The relative angles of these three bones to the tibia in the z axis were 24.51º, 09.32º, and 9.41º, respectively.

Alignment of Metatarsal Bones Relative to Tibia

Results of the relative angles between the metatarsal bones and tibia showed that there was a higher x-axis angle value in comparison with the other axes, especially for the first and second metatarsal bones (Table I). This is due to the malalignment of the metatarsal bones in the two osseous columns, which translated medially along with the other tarsal bones (talus, calcaneus, cuboid and navicular bones, and lateral, middle, and medial cuneiforms). In the metatarsal bones, the x axis was oriented medially, y axis was directed inferiorly and anteriorly, and the z axis was oriented in the vertical direction in general. Results also showed that the x axis was oriented medially, y axis was oriented inferiorly, and z axis was oriented in the vertical direction in the lower end

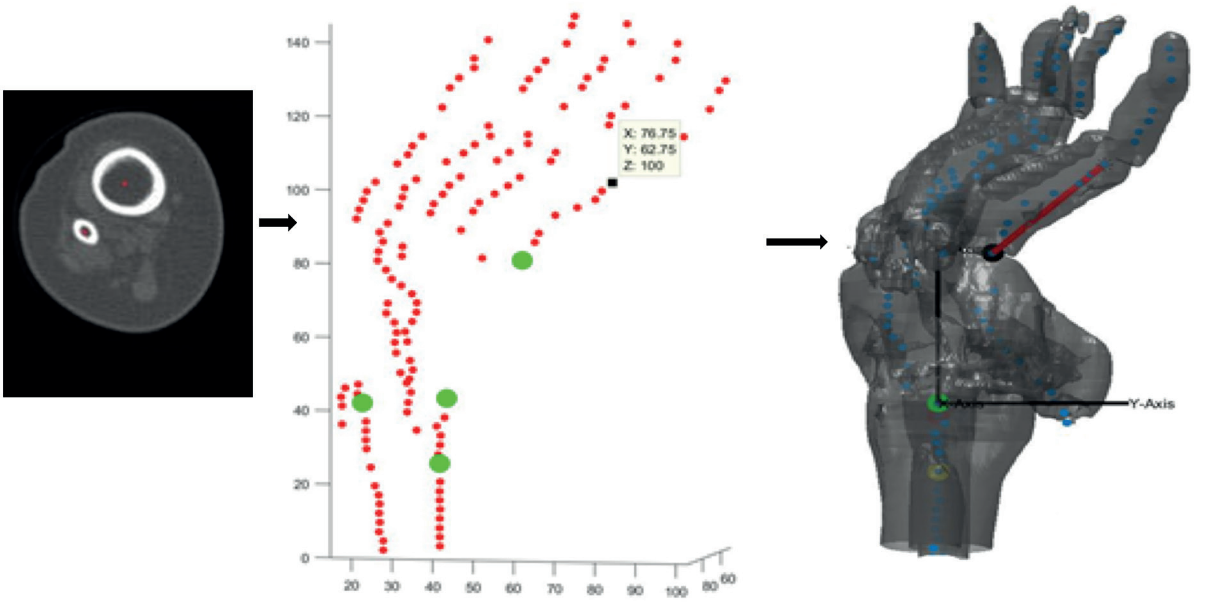

Figure 2. Processing of 3D bone model of severe clubfoot from 2D slices of CT images.

of tibia (Figure 3a). In addition, relative angle of the fifth metatarsal bone was the smallest among all metatarsal bones in all axes (30.37º). Relative angles of metatarsal bones to tibia can be used to compare the different levels of clubfoot severity with a normal foot.

Alignment of Proximal, Middle, and Distal Phalangeal Bones Relative to Lower End of Tibia

Rotation of the proximal phalangeal bones relative to tibia was objectively measured and the results showed a higher rotation angle about the y axis in comparison to the other axes of rotation. Of these phalangeal bones, the fifth proximal phalangeal bone had a greater y axis angle (91.02º), followed by that of the second and third proximal phalange bones of 86.35º and 80.07º, respectively. On the other hand, the z axis angle of all the proximal phalanges was lower than the angle of other axes of the proximal phalangeal bones. This smaller z axis angle indicates that the proximal phalangeal bones were more plantar flexed and had an adducted position relative to the lower leg. To measure the angles at the middle phalanges, the orientations of the second to fifth toes to the tibia were quantified. Among the middle phalangeal bones, a higher rotation angle was observed in the x axis of the fifth middle phalanx relative to the tibia (98.05º), followed by the fifth middle phalanx of little toe in the y axis (87.18º), and the second and third middle phalanges of 70.91º and 72.74º in the x axis, respectively. The smallest relative angle was observed in the fifth middle phalanx (8.53º), which was more deviated than the other phalangeal bones. In the y axis, the rotation angles of the third and fourth middle phalangeal bones were 41.08º and 47.19º, respectively. Among the proximal and distal phalangeal bones in relation to the tibia, the third (112.86º) and fourth (106º) distal phalangeal bones were more deviated in the direction of the x axis. Figure 3e shows the position of the first distal phalanx in relation to the lower end of tibia. Results indicated that the third and fourth distal phalanges were rotated more medially. The rotation angle of the fifth distal phalanx was smallest in the x-axis direction (65.47º). The Z axis was the longest axis and demonstrated the smallest moment of inertia in the distal phalangeal bones. The rotation angles of the third and fourth distal phalangeal bones were less in the z axis compared to the first, second, and fifth distal phalangeal bones.

Discussion

A 3D model for severe clubfoot was developed from 2D images, which was obtained from CT scanning, to quantify the severity and alignment or position of bones in a severe clubfoot. To create the 3D model of the clubfoot, MATLAB

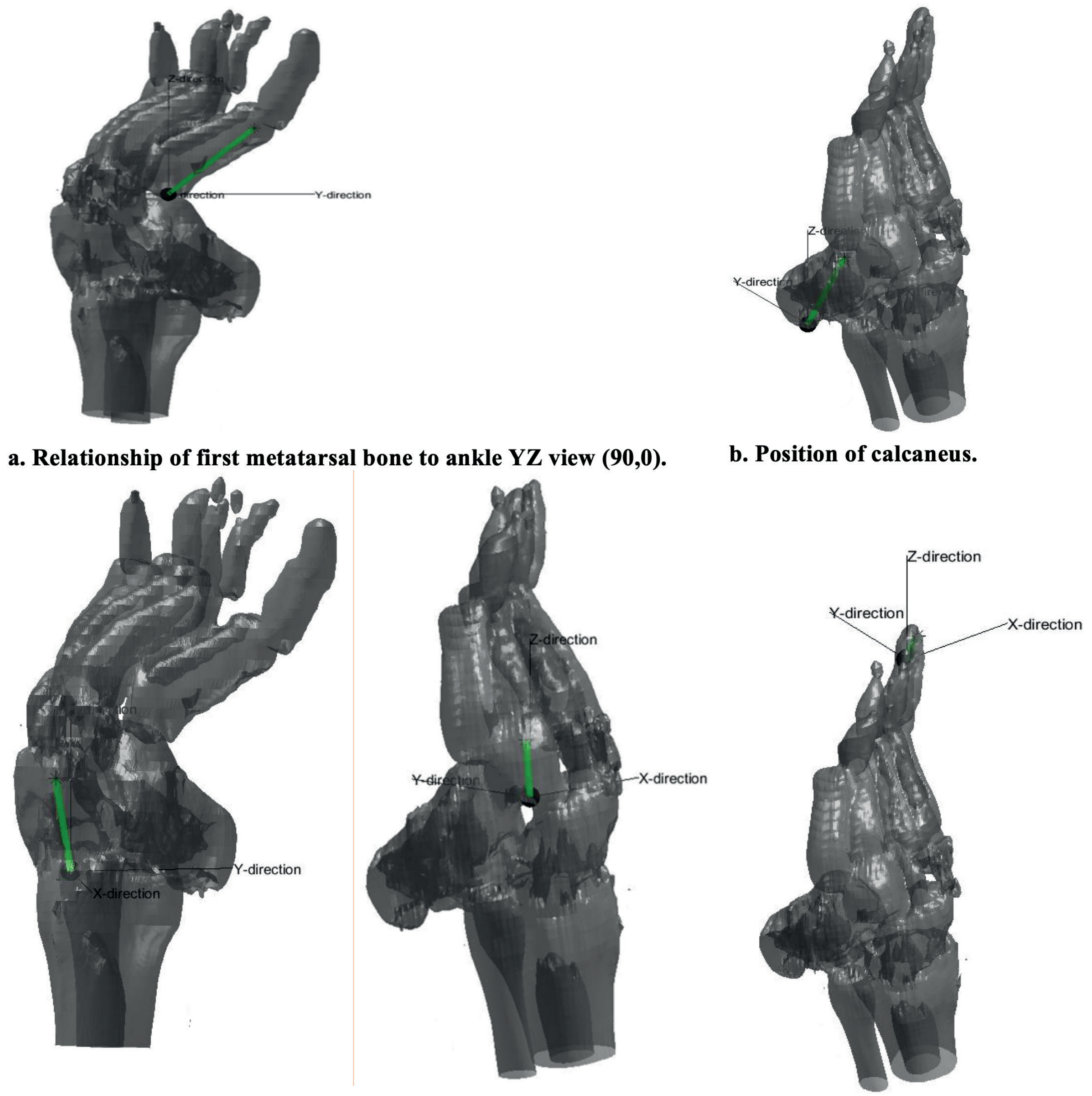

a. Relationship of first metatarsal bone to ankle YZ view (90,0). **b. Position of calcaneus.**

c. Position of the talus. **d. Position of cuboid.** **e. Position of first distal phalanx.**

Figure 3. Position and alignment of first metatarsal, calcaneus, talus, cuboid and first distal phalanx in relative to the tibia in the clubfoot.

program was used to automatically calculate the angle of each bone of the foot. In this study, the x, y, and z coordinate axis angles were documented for each bone of the foot (talus, calcaneus, cuboid, metatarsal, and phalangeal bones) from the 3D model of the clubfoot, to objectively determine the relative angles between the bones of interest. The relative angles between the ankle and bones of interest were used to objectively determine the deviation of the bones in the clubfoot.

Clubfoot is a complex three-dimensional deformity that involves malalignment of the medial and lateral osseous columns. Therefore, it is important to assess the medial and lateral osseous columns and their relationship with the lower leg for a better understanding of the clubfoot anatomy and the relationship of each bone in the foot and ankle. Recently, a number of imaging, functional, and radiological methods have been used to evaluate clubfoot[32-37]. However, the use of conventional radiography or CT scanning may not be the best way to evaluate the clubfoot structure. This is because CT images are only useful for examining pathological anatomy of the foot in 2D. Therefore, it is difficult to assess the morphology, alignment, and orientation of each foot bone and all of the hindfoot joints thoroughly[8,32]. Another disadvantage of using 2D images is that they may not be reliable to provide accurate information on the alignment and morphology of the tarsal bones which are not ossified in newborn babies[20,38-39]. Moreover, previous studies have mostly focused on evaluating the relationships among the talus, navicular, calcaneus and cuboid bones through imaging[32,40-43]. Therefore, to the best of our knowledge, there were no studies that focus on the clubfoot and examine the alignment between the ankle and bones of the foot.

Camacho et al[44] were the first to use Euler angle rotations to describe the relationships among several bones (first and second metatarsal, navicular, and cuboid bones) and the talus in a normal foot. In addition, Windisch et al[1] suggested that the development of a 3D model helps to provide a better understanding of the complexities of clubfoot including deformation of talus and calcaneus. Based on these studies, we first reconstructed CT image slices into 3D images to examine the alignment of tarsal, metatarsal, and phalangeal bones of the foot, and the relationships between the ankle joint and bones of the foot in the present study. The difference in angle measurements of the bones of foot can be used to quantify the deformation and severity of clubfoot, and to accurately and objectively examine the alignment of each bone in the foot. The difference in the angle measurements can also be used to compare a splinted and a normal foot to evaluate the progression of clubfoot associated with treatment. Generally, three planes (sagittal, frontal and coronal planes), and the transverse planes are used to assess the movement directions of the foot (plantar flexion and dorsiflexion - sagittal plane; abduction and adduction - coronal or frontal plane; and inversion and eversion (transverse plane)). Pekindil et al[45] examined the talocalcaneal angle in the sagittal plane, internal rotation of the talar head and neck-axis, and internal rotation of the calcaneal-axis, transverse talar neck and head, external rotation in the posterior side of the calcaneus, and calcaneus angle in the clubfoot[45]. The bone-to-bone relationships in the foot varied in different types of foot and the differences can be measured by Cardan angles[46]. In the present study, the difference in the orientation of the bones in foot was measured by the angular deviations between the bones of interest to the ankle. This study has some limitations, for example, only the relative position of the tarsal bones to the tibia was measured. The relative position of the tarsal bones to the calcaneus and talus were not determined. In addition, this was a single-case study. We used one CT scan to develop a surface model and determine the bone-to-bone relationships. Therefore, further studies are necessary to examine the relative angle of each bone to the calcaneus and talus with larger sample size. Results can also be compared with normal foots. Changes of the relative angles of foot bones after weekly casting intervention for clubfoot may also be measured in future studies.

Conclusions

This study presented a new methodology to develop a 3D surface model of severe clubfoot from 2D slices of CT images. It also provided some basic information for the development of an objective method to quantify the bone-to-bone relationships in clubfoot deformity. Specifically, to determine the bone-to-bone relationships, relative angles between bones of the ankle and foot complex were measured and used for evaluating the severity of clubfoot. This novel method may also be used to assess other pathological conditions of the foot such as pes cavus and pes planus.

Conflict of Interest

The Authors declare that they have no conflict of interests.

Acknowledgements

The work is supported by PolyU funding entitled "Development of 3D Spacer Fabrics to Prevent Surgical Pressure Ulcers" (G-YBV3). The project is also supported by FEIT PhD Post Thesis Publication Scholarship-University of Technology of Sydney, Australia.

References

1) Windisch G, Salaberger D, Rosmarin W, Kastner J, Exner GU, HaldiÐBrändle V, Anderhuber F. A model for clubfoot based on micro-CT data. J Anat 2007; 210: 761-766.

2) Mejabi JO, Esan O, Adegbehingbe OO, Asuquo JE, Akinyoola AL. A prospective cohort study on comparison of early outcome of classical Ponse-

ti and modified Ponseti post tenotomy in clubfoot management. Ann Med Surg (Lond) 2017; 24: 34-37.

3) Miedzybrodzka Z. Congenital talipes equinovarus (clubfoot): a disorder of the foot but not the hand. J Anat 2003; 202: 37-42.

4) Dobbs MB, Gurnett CA. Update on clubfoot: etiology and treatment. Clin Orthop Relat Res 2009; 467: 1146-1153.

5) Aurell Y, Andriesse H, Johansson A, Jonsson K. Ultrasound assessment of early clubfoot treatment: a comparison of the Ponseti method and a modified Copenhagen method. J Pediatr Orthop B 2005; 14: 347-357.

6) Cosma D, Vasilescu DE. A clinical evaluation of the Pirani and Dimeglio idiopathic clubfoot classifications. J Foot Ankle Surg 2015; 54: 582-585.

7) Herd F, Macnicol M, Abboud R. The need for biomechanical evaluation in the assessment of clubfoot. Foot 2004; 14: 72-76.

8) Johnston CE, Hobatho MC, Baker KJ, Baunin C. Three-dimensional analysis of clubfoot deformity by computed tomography. J Pediatr Orthop 1995; 4: 39-48.

9) Kamegaya M, Shinohara Y, Kuniyoshi K, Moriya H. MRI study of talonavicular alignment in clubfoot. J Bone Joint Surg Br 2001; 83: 726-730.

10) Yeung EH, Li YH, Ng ON, Chow W. Radiographic assessment of congenital talipes equinovarus: strapping versus forced dorsiflexion. J Orthop Surg (Hong Kong) 2005; 13: 253-258.

11) Dyer PJ, Davis N. The role of the Pirani scoring system in the management of club foot by the Ponseti method. J Bone Joint Surg Br 2006; 88: 1082-1084.

12) Ganesan B, Luximon A, Al-Jumaily AA, Yip J, Gibbons PJ, Chivers A. Developing a three-dimensional (3D) assessment method for clubfoot – a study protocol. Front Physiol 2018; 8: 1098.

13) Gao R, Tomlinson M, Walker C. Correlation of Pirani and Dimeglio scores with number of Ponseti casts required for clubfoot correction. J Pediatr Orthop 2014; 34: 639-642.

14) Anand A, Sala DA. Clubfoot: etiology and treatment. Indian J Orthop 2008; 42: 22.

15) Bensahel H, Huguenin P, Themar-Noel C. Functional anatomy of clubfoot. J Pediatr Orthop 1983; 3: 191-195.

16) Siapkara A, Duncan R. Congenital talipes equinovarus a review of current management. J Bone Joint Surg Br 2007; 93: 1160-1164.

17) Pinto JA, Hernandes AC, Buchaim TP, Chertman C, Yamane PC, da Rocha Corrêa Fernandes A. Radiographic abnormalities of the talus in patients with clubfoot after surgical release using the mckay technique. Acta Ortop Bras 2008; 16: 270-274.

18) Epeldegui T. Deformity of talus and calcaneous in congenital clubfoot: an anatomical study. J Pediatr Orthop B 2012; 21: 10-15.

19) Flinchum D. Pathological anatomy in talipes equinovarus. J Bone Joint Surg Am 1953; 35-A: 111-114.

20) Itohara T, Sugamoto K, Shimizu N, Ohno I, Tanaka H, Nakajima Y, Sato Y, Yoshikawa H. Assessment of talus deformity by three-dimensional MRI in congenital clubfoot. Eur J Radiol 2005; 53: 78-83.

21) Cahuzac JP, Baunin C, Luu S, Estivalezes E, Sales de Gauzy J, Hobatho MC. Assessment of hindfoot deformity by three-dimensional MRI in infant clubfoot. J Bone Joint Surg Br 1999; 81: 97-101.

22) Ippolito E, Dragoni M, Antonicoli M, Farsetti P, Simonetti G, Masala S. An MRI volumetric study for leg muscles in congenital clubfoot. J Child Orthop 2012; 6: 433-438.

23) Bhargava SK, Tandon A, Prakash M, Arora SS, Bhatt S, Bhargava S. Sonographic evaluation of clubfoot: a comparative study. Indian J Orthop 2012; 46: 229-235.

24) Kruse L, Gurnett CA, Hootnick D, Dobbs MB. Magnetic resonance angiography in clubfoot and vertical talus: a feasibility study. Clin Orthop Relat Res 2009; 467: 1250-1255.

25) Duce SL, D'Alessandro M, Du Y, Jagpal B, Gilbert FJ, Crichton L, Barker S, Collinson JM, Miedzybrodzka Z. 3D MRI analysis of the lower legs of treated idiopathic congenital talipes equinovarus (clubfoot). PLoS One 2013; 8: e54100.

26) Merrill LJ, Gurnett CA, Siegel M, Sonavane S, Dobbs MB. Vascular abnormalities correlate with decreased soft tissue volumes in idiopathic clubfoot. Clin Orthop Relat Res 2011; 469: 1442-1449.

27) Farsetti P, Dragoni M, Ippolito E. Tibiofibular torsion in congenital clubfoot. J Pediatr Orthop B 2012; 21: 47-51.

28) Brockett CL, Chapman GJ. Biomechanics of the ankle. Orthop Trauma 2016; 30: 232-238.

29) Kaplan EB. Comparative anatomy of the talus in relation to idiopathic clubfoot. Clin Orthop1972; 85: 32-37.

30) Baghdadi T, Bagheri N, Najafi A, Mansouri P, Farzan M. Ponseti casting method in idiopathic congenital clubfoot and its correlation with radiographic features abstract. Arch Bone Jt Surg 2017; 5: 168-173.

31) Radler C, Manner HM, Suda R, Burghardt R, Herzenberg JE, Ganger R, Grill F. Radiographic evaluation of idiopathic clubfeet undergoing Ponseti treatment. J Bone Joint Surg Am 2007; 89: 1177-1183.

32) Ippolito E, Fraracci L, Farsetti P, De Maio F. Validity of the anteroposterior talocalcaneal angle to assess congenital clubfoot correction. AJR Am J Roentgenol 2004; 182: 1279-1282.

33) Downey DJ, Drennan JC, Garcia JF. Magnetic resonance image findings in congenital talipes equinovarus. J Pediatr Orthop 1992; 12: 224-228.

34) Grayhack JJ, Zawin JK, Shore RM, Trombino LJ, Poznanski AK, Carroll NC. Assessment of calcaneocuboid joint deformity by magnetic resonance

imaging in talipes equinovarus. J Pediatr Orthop B 1995; 4: 36-38.

35) Moritani T, Aihara T, Oguma E, Shimanuki Y, Takano H, Sato M. MR evaluation of talonavicular angle in congenital talipes equinovarus. Clin Imag 2000; 24: 243-247.

36) Pirani S, Zeznik L, Hodges D. Magnetic resonance imaging study of the congenital clubfoot treated with the Ponseti method. J Pediatr Orthop 2001; 21: 719-726.

37) Ippolito E, Fraracci L, Caterini R, Di Mario M, Farsetti P. A radiographic comparative study of two series of skeletally mature clubfeet treated by two different protocols. Skeletal Radiol 2003; 32: 446-453.

38) Desai S, Aroojis A, Mehta R. Ultrasound evaluation of clubfoot correction during Ponseti treatment: a preliminary report. J Pediatr Orthop 2008; 28: 53-59.

39) Herzenberg JE, Carroll NC, Christofersen MR, Lee EH, White S, Munroe R. Clubfoot analysis with three-dimensional computer modeling. J Pediatr Orthop 1988; 8: 257-262.

40) Hubbard AM, Meyer JS, Davidson RS, Mahboubi S, Harty MP. Relationship between the ossification center and cartilaginous anlage in the normal hindfoot in children: study with MR imaging. Am J Roentgenol 1993; 161: 849-853.

41) Farsetti P, De Maio F, Russolillo L, Ippolito E. CT study on the effect of different treatment protocols for clubfoot pathology. Clin Orthop Relat Res 2009; 467: 1243-1249.

42) Itohara T, Sugamoto K, Shimizu N, Ohno I, Tanaka H, Nakajima Y, Sato Y, Yoshikawa H. Assessment of talus deformity by three-dimensional MRI in congenital clubfoot. Eur J Radiol 2005; 53: 78-83.

43) Itohara T, Sugamoto K, Shimizu N, Ohno I, Tanaka H, Nakajima Y, Sato Y, Yoshikawa H. Assessment of the three-dimensional relationship of the ossific nuclei and cartilaginous anlagen in congenital clubfoot by 3-D MRI. J Orthop Res 2005; 23: 1160-1164.

44) Camacho DL, Ledoux WR, Rohr ES, Sangeorzan BJ, Ching RP. A three-dimensional, anatomically detailed foot model: a foundation for a finite element simulation and means of quantifying foot-bone position. J Rehabil Res Dev 2002; 39: 401-410.

45) Pekindil G, Aktas S, Saridogan K, Pekindil Y. Magnetic resonance imaging in follow-up of treated clubfoot during childhood. Eur J Radiol 2001; 37: 123-129.

46) Ledoux WR, Rohr ES, Ching RP, Sangeorzan BJ. Effect of foot shape on the three-dimensional position of foot bones. J Orthop Res 2006; 24: 2176-2186.